



Scholars Research Library

Der Pharma Chemica, 2015, 7(4):155-163
(<http://derpharmachemica.com/archive.html>)



ISSN 0975-413X
CODEN (USA): PCHHAX

Molecular docking, pharmacophore modeling and 3D-QSAR approach on a series of piperidone derivatives as potential anticancer agents by targeting the enzyme VEGFR-2 tyrosine kinase

Revathi Rajappan¹, Venkatesha Perumal Ramachandran², Karkala Sreedhara Ranganath Pai³, Govindakarnavar Arunkumar⁴, Josula Venkata Rao⁵, Hitesh Jagani⁵ and Suvarna Ganesh Kini^{1*}

¹Department of Pharmaceutical Chemistry, Manipal College of Pharmaceutical Sciences, Manipal University, Manipal, Karnataka, India

²Medicinal Chemistry Department, College of Pharmacy, Qassim University, Qassim, Saudi Arabia

³Department of Pharmacology, Manipal College of Pharmaceutical Sciences, Manipal University, Manipal, Karnataka, India

⁴Manipal Centre of Virus Research, Manipal University, Manipal, Karnataka, India

⁵Department of Pharmaceutical Biotechnology, Manipal College of Pharmaceutical Sciences, Manipal University, Manipal, Karnataka, India

ABSTRACT

For a series of piperidone derivatives with anticancer activity against MCF7 cell lines pharmacophore modeling was performed by using PHASE, Partial least-squares (PLS) method was used to explore conformational space. All docking studies for the target compounds with VEGFR-2 tyrosine kinase were performed using GLIDE programme (Schrödinger Inc., USA). Statistically significant 3D-QSAR model was obtained through the pharmacophore hypothesis. A four-point pharmacophore with one hydrophobic (H), one hydrogen bond donor with positive ionic charge (P), and two aromatic rings (R) as pharmacophore features was developed with a correlation coefficient of r^2 0.7586 and with a correlation coefficient of q^2 0.532 for training set and test set of compounds, respectively with the excellent predictive power. The results provide insights that will facilitate the further structural modification of these anticancer agents for better activity, and may prove beneficial for lead optimization and in silico screening in future.

Keywords: Molecular docking, pharmacophore modeling, 3D QSAR; piperidone, anticancer activity, VEGFR-2 tyrosine kinase.

INTRODUCTION

In tumor angiogenesis, the vascular endothelial growth factor (VEGF) is involved as one of the most important pro-angiogenic factor [1]. Hence, for the inhibition of tumor angiogenesis blockade of the VEGF/VEGFR-signaling is considered as an attractive therapeutic target [2]. There are six subgroup of proteins in VEGF family. They are placenta growth factor and VEGF-A, B, C, D, E. The biological effects of these proteins are exerted by binding and activation of receptors like VEGFR1, VEGFR2 and VEGFR3. Among these, VEGF-A-induced angiogenesis in endothelial cells is transduced by the major receptor VEGFR2 [3]. Auto phosphorylation of the VEGFR2 receptor is resulted by the binding of VEGF-A to the receptor which leads to the activation of downstream signaling molecules

including focal adhesion kinase (FAK), 3-phosphoinositide-dependent kinase 1 (PDK1), phosphoinositide 3-kinase, Proto-oncogene tyrosine-protein kinase Src and Protein Kinase B (PKB), extracellular signal-regulated kinases (ERK) [4]. Cell survival and motility has been regulated by the activation of ERK pathway [5]. Cell migration, proliferation, and angiogenesis have been promoted by the activation of tyrosine-protein kinase Src by VEGFR2 [6,7].

In numerous solid tumors with aggressive disease the most closely associated angiogenic factor is VEGF, which is involved in oncogene activation [8] and loss of tumor suppressor gene function [9]. The over expression of VEGF by tumor cells occurs frequently [10]. In many human cancers poor prognosis and increased micro vessel counts are correlated with elevated VEGF level [11]. Furthermore, in newly formed blood vessels, VEGF functions as a potent antiapoptotic factor for endothelial cells [12]. The tyrosine kinase (RTK) VEGF receptor is located on endothelial cells [13]. Its expression levels are only increased in pathologic states (neovascularization). VEGFR-2 has an intracellular split tyrosine kinase domain, an extracellular VEGF-binding domain and single membrane-spanning domain.

Inhibitions of VEGFR are currently being assessed in clinical trials with a variety of approaches. These include small molecule inhibitors, monoclonal antibodies targeting VEGFR and soluble receptors that sequester VEGF [14]. However, some adverse effects has been resulted with most of these inhibitors such as bleeding complications [15], and hence the need for new VEGFR signaling cascade inhibitors with less toxicity, prompted us to evaluate a series of piperidone derivatives by carrying out the molecular modeling studies in an effort to discover more potent VEGFR inhibitors with low toxicity.

For the prediction of biological activities the quantitative structure–activity relationship (QSAR) approach is largely widespread and very useful tool, particularly in drug design [16,17]. In this approach the changes in their molecular features were correlated with the variations in the properties of the compounds [7]. This study was aimed to obtain the interaction of our compounds with the active residue of the receptor (VEGFR2) and also the predictive three-dimensional QSAR (3D-QSAR) models to elucidate the structural features of piperidone derivatives required for VEGFR inhibition. This will provide better tools for the rational design of promising VEGFR inhibitors with more therapeutic efficacy and safety.

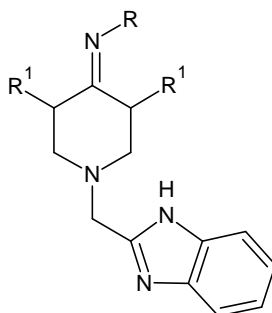
MATERIALS AND METHODS

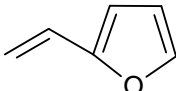
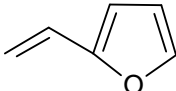
Schrödinger Inc., USA software was used to carry out the present the study .Pharmacophore modeling was performed by using PHASE, running on Red Hat Linux WS 5.0.

Data set

As a continuation of our previous studies, in this study 22 compounds having anticancer activity [18] are used to construct 3D QSAR model. The biological activity data was in the form of IC_{50} and these values were converted into pIC_{50} using the formula, $pIC_{50} = -\log IC_{50}$. The test compounds structures with their actual and predicted activities are presented in Table 1.

Table 1 Experimental and predicted activity of the piperidone derivatives used in training and test sets for VEGFR-2 inhibition using Model-1 and their Glide dock Score.



Compd.	R	R ¹	IC ₅₀ (μM/ml)	pIC ₅₀ (μM/ml)		Residual	Glide Dock Score
				Exp.	Pred.		
S1	=O (=N-R)	H	0.62	6.207	6.28	-0.073	-4.075
S2	-OH	H	0.35	6.455	6.34	0.115	-5.330
S3	-NH ₂	H	0.27	6.568	6.35	0.218	-5.865
S4	-C(=S)-NHNH ₂	H	0.125	6.903	6.93	-0.027	-6.766
S5	-C(=S)-NHNH-OH	H	2.14	5.669	5.95	-0.281	-3.928
S6	<i>p</i> -F-C ₆ H ₄	H	0.08	7.096	6.68	0.416	-6.882
S7	-NH-C ₆ H ₄	H	0.28	6.552	6.31	0.242	-5.336
S8	<i>o,p</i> -OCH ₃ -C ₆ H ₃	H	0.17	6.769	6.79	-0.021	-6.536
S9	<i>o,m</i> -CH ₃ -C ₆ H ₃	H	0.18	6.744	6.53	0.214	-6.323
S10	<i>o</i> -CH ₃ - <i>m</i> -Cl-C ₆ H ₃	H	0.20	6.698	6.6	0.098	-6.031
S11	<i>o,p</i> -Cl-C ₆ H ₃	H	0.45	6.346	6.32	0.026	-5.005
S12	<i>o,p</i> -F-C ₆ H ₃	H	0.41	6.387	6.56	-0.173	-5.032
S13	-C(=NH)-NH ₂	H	2.75	5.560	5.49	0.07	-4.372
S14	-C ₆ H ₅	H	1.7	5.769	6.34	-0.571	-4.420
S15	<i>p</i> -Cl-C ₆ H ₄	H	0.36	6.443	6.5	-0.057	-5.442
S16	-C(=O)-NH ₂	H	0.91	6.040	6.41	-0.37	-4.683
S17	<i>o,p</i> -NO ₂ -C ₆ H ₃	H	0.98	6.008	5.84	0.168	-4.160
S18	-C(=S)-NH ₂	H	1.74	5.759	5.84	-0.081	-4.018
S19	-OCH ₃	H	0.38	6.420	6.33	0.09	-5.122
S20	-C(=O)-NHNH ₂	H	0.32	6.494	6.37	0.124	-5.269
B1	=O (=N-R)		0.61	6.214	6.30	-0.086	-4.307
B2	-OH		0.56	6.251	6.34	-0.089	-5.003

Ligand preparation

All molecules were in Maestro and were prepared using LigPrep with the optimized potentials for liquid simulations (OPLS) 2005 force field. Conformational space was explored through the combination of Monte-Carlo Multiple Minimum (MCM) / Low Mode (LMOD) with maximum number of conformers 1000 per structure and minimization steps 100. Each minimized conformer was filtered through a relative energy window of 50 kJ/mol and redundancy check of 2 Å in the heavy atom positions [19].

Training and test set selection

Data set were divided randomly by choosing 16 compounds in training set and 6 compounds in test set to maintain the 3:1 ratio. While dividing the test and training set, the even distribution of structurally varying compounds has been ascertained with a wide range of pIC₅₀ value in both test and training set. The most active and inactive were kept in the training set [20]. PLS factor 2 is used for the model generation.

Pharmacophore sites

The common pharmacophore hypothesis (CPH) was performed by PHASE. Common pharmacophoric features were then identified from a set of variants that define a possible pharmacophore using a tree-based partitioning algorithm with maximum tree depth of four with the requirement that all actives must match. After applying default feature definitions to each ligand, common pharmacophores were generated using a terminal box of 1 Å. A set of SMARTS patterns were used to represent the positions of pharmacophore sites (feature definitions) internally. A set of chemical structure patterns which defines the pharmacophore feature are specified as SMARTS queries. The physical characteristics of the site were defined by one of three possible geometries. They are: 1). Point: in the SMARTS query, the site is located on a single atom. 2). Vector: in the SMARTS [21] query, the site is located on a single atom as like point, but it will be assigned based on one or more vectors originating from that atom and according to directionality. 3). Group: in the SMARTS query the site is located on the group of atoms at the centroid. To create pharmacophore sites a default setting having a hydrogen bond acceptor (A), hydrogen bond donor (D), hydrophobic (H), negative (N), positive (P), and aromatic ring (R) was used.

Scoring hypothesis

Scoring function was used to examine these CPH. Overall maximum root mean square deviation (RMSD) value of 1.2 Å was used to obtain the better alignment of the ligands. Quality of alignment is measured by survival score which is represented as follows.

$S = W_{site}S_{site} + W_{vec}S_{vec} + W_{vol}S_{vol} + W_{sel}S_{sel} + W_{mrew}$ where W = weights and S = scores, S_{site} = alignment score; S_{vec} = vector score S_{vol} = volume score and S_{sel} = selectivity score. W_{site} , W_{vec} , W_{vol} , and W_{rew} have default values of 1.0, while W_{sel} has a default value of 0.0. In hypothesis generation, default values have been used. W_{mrew} represents reward weights defined by $m-1$, where m is the number of actives that match the hypothesis.

With respect to the activity of ligand, scoring of pharmacophore was conducted using default parameters for volume, vector, and site terms. To explain the Structural activity relationship the entire molecular structure has to be considered as in atom-based QSAR whereas in Pharmacophore based QSAR the ligand features beyond the pharmacophore model is not considered, such as possible steric clashes with the receptor. A molecule is considered as a set of overlapping Vanderwaals spheres in atom based QSAR. Each sphere (atom) is placed into one of following six categories. They are carbons, C–H hydrogens and halogens, are classified as non-polar / hydrophobic (H); hydrogens attached to polar atoms are classified as hydrogen bond donors (D); atoms with an explicit positive ionic charge are classified as positive ionic (P); atoms with an explicit negative ionic charge are classified as negative ionic (N); non-ionic atoms are classified as electron-withdrawing (W); and all other types of atoms are classified as miscellaneous (X).

For the development of QSAR, in a regular grid of training set Vanderwaals models of the ligand training set molecules were placed that occupies the cube. This binary-valued occupation patterns can be used as independent variables. Using the 16 membered training set with a grid spacing of 1.0 Å, pharmacophore based QSAR models for all hypotheses were generated and by predicting the activities of the six test set compounds the best QSAR model was validated.

Building 3D-QSAR models using PLS analysis

To a CPH associated with a single reference ligand, the test molecules with varying activity have been aligned to develop QSAR models. These pharmacophore-based 3D-QSAR models with random seed value of zero, grid spacing 1.0 Å and 1–5 PLS factors were build when all hypotheses were successfully generated. For the top ten scoring hypothesis, statistics were performed on the correlation of actual activity with predicted activity by the default hypothesis scoring functions. The QSAR model was obtained by PLS regression analysis. The dependent variable was the inhibitory activity and the independent variables were eliminated by using ‘a’ ‘t’ value filter and a default value of 2.0 because to make small changes in the training set composition their regression coefficients are too sensitive. The maximum number of PLS factors were 12. In PHASE QSAR models distinct training and test sets were used but not the internal cross-validation techniques, since PHASE supports only external validation. The validation of each of the developed 3D-QSAR models were carried out by predicting activities of six test set molecules (q^2). Pearson-R value is used to measure the predictive ability of the models. By using 1–5 PLS factors the run was performed to overcome the over-fitting problem, in which the experimental error was approximately equal to the standard deviation of regression. The strength of the resulting 3D QSAR model was checked and also the comparison of the models from different hypothesis was carried out by the stability value.

Docking studies

The molecular docking studies were carried out with VEGFR-2 tyrosine kinase binding pocket by using the tool, GLIDE (Schrödinger Inc., USA) (2008). Then VEGFR-2 tyrosine kinase crystal structure used in the present study was downloaded from the protein data bank (PDB ID: 1YWN). Protein preparation was performed by using the Maestro software (Schrödinger) and alignment was performed using the protein alignment module (Prime, Schrödinger). Bond orders and formal charges were added for hetero groups and hydrogens were added to all atoms in the system. Water molecules of crystallization were removed from the complex except in the active site. Protein Preparation module in Maestro was used to perform a brief relaxation on structure with the “Refinement Only” option. This is a procedure consisting of two-part which is optimization of thiol and hydroxyl torsions in the first part followed by an all-atom constrained minimization carried out with Impact Refinement module (Impref) using

the OPLS-2005 force field minimized [22] to alleviate steric clashes that may exist in the original PDB structures. The minimization was terminated when the RMSD reached a cut off of 0.30 Å.

The prepared ligands were docked against the protein VEGFR-2 kinase. All the calculations for docking were performed using the “Extra precision” (XP) mode (Glide, Schrödinger). Final scoring is then carried out on the energy-minimized poses. The minimized poses are rescored using Schrödinger’s proprietary Glide Score (G Score) scoring function. G Score is a modified version of ChemScore, but includes a steric-clash term and adds buried polar terms devised by Schrödinger to penalize electrostatic mismatches. All docking computations were carried out with the Linux OS (Red Hat Enterprise WS 5.0).

RESULTS AND DISCUSSION

Tree-based partition algorithms were used to identify the CPH using the training set. Based on the observed activity, the dataset was divided into active and inactive sets to find out the CPH. The ligands are active if the $\log IC_{50}$ is $\geq 6.7 \mu\text{M/ml}$ and inactive if $\leq 6 \mu\text{M/ml}$. Number of CPH were reported with maximum of four features which was allowed to develop hypothesis based on sites and they are common in all 22 molecules. There were totally 144 hypothesis; among that five hypothesis were selected based on the survival score for molecular alignment. PLS analysis was carried out using 12 factors with a grid spacing 1 Å to derive five regression models. The best fitted Model-I HPRR.1 ($r^2 = 0.7586$, $q^2 = 0.532$, $F = 20.4$) and its regression summary are given in Table 2. The pharmacophore hypothesis for model-I is depicted in Fig. 1. Hydrophobic site is indicated by the green ball, hydrogen bond donor site is indicated by blue ball. The R (ring) feature of the pharmacophore is demonstrated by the brown ring. (Fig. 1). For Models 1–5, their statistical scores are listed in Table 2.

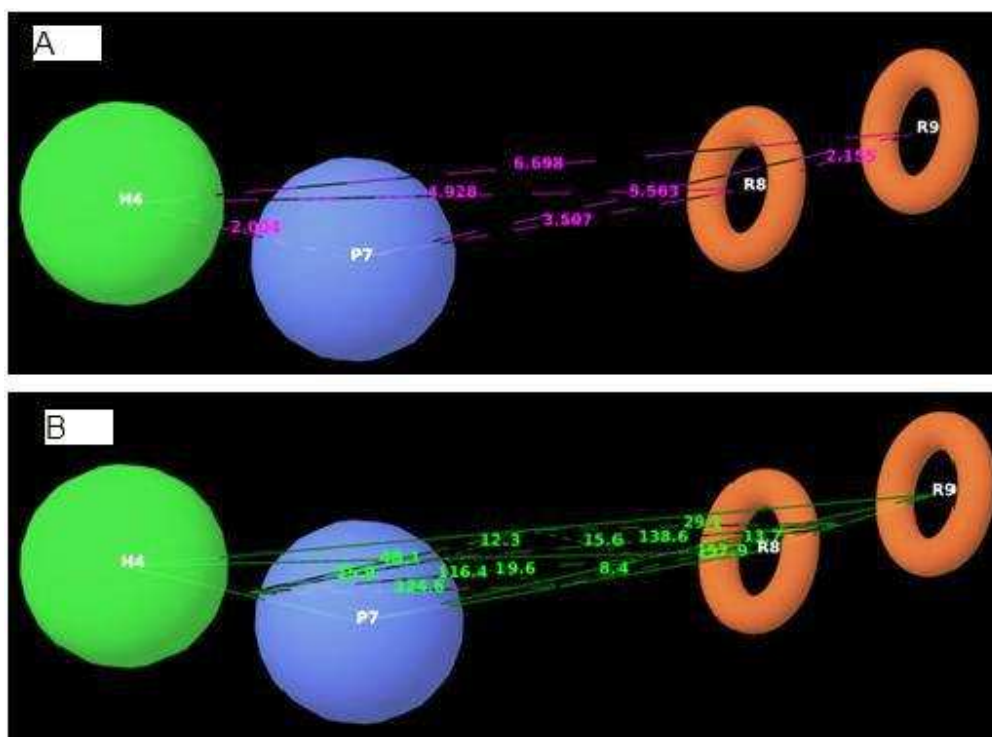


Figure 1: Pharmacophore distances (A) and angles (B) between pharmacophoric sites. Pharmacophore hypothesis (HPRR), where the green ball shows hydrophobic site, blue ball indicates hydrogen bond donor with positive charge while the brown ring demonstrates the R (ring) feature.

Table 2 Statistical data for best QSAR Model-1 for piperidone derivatives by the PLS method

Hypothesis ID	Factor	SD	R ²	F	Stability	RMSE	Q ²	Pearson R
HPRR.1	12	0.2223	0.7586	20.4	0.7033	0.2509	0.532	0.7938
DHPR.6	12	0.3623	0.7317	19.16	0.6727	0.3004	0.4912	0.7356
DHPR.4	12	0.4712	0.6932	16.53	0.6456	0.3235	0.4234	0.7122
DHPR.12	12	0.6015	0.6148	15.29	0.5910	0.4816	0.3763	0.6314
DHPR.10	12	0.6194	0.5950	13.18	0.5823	0.5108	0.3096	0.5909

R² = Coefficient of determination; Q² = cross validated R²; F = F test score; Pearson R = correlation between experimental and predicted activity for the test set.

GLIDE (Schrödinger Inc., USA) (2006) was used to carry out the docking study for the test molecules against the enzyme VEGFR-2 tyrosine kinase (PDB ID: 1YWN), which was obtained from the protein data bank PDB. Molecular modeling was carried out by positioning our compounds in the reference ligand's binding site. Then it was subjected to minimization and dynamics. The binding mode of test molecules and the reference ligand were compared by docking the reference ligand and test molecules into the enzyme VEGFR-2 tyrosine kinase.

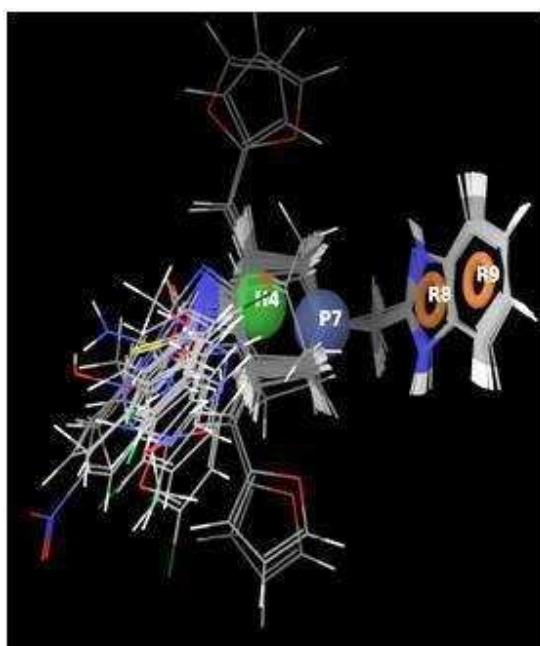


Figure 2: The common pharmacophore based alignment of all molecules in 3D QSAR

Docking studies have shown that the N- of the benzimidazole ring interacts with H-atom of the amino acid backbone of GLU-883 through a hydrogen bond (Fig. 3 & 4). These interactions reveal the significance of nitrogen atom for inhibitory capacity. The nitrogen in the substituent at the 4th position of piperidone ring which is surrounded by the hydrophobic residues like ALA-854, CYS-917, LEU-1033, PHE-916, LEU-838, and VAL-846. The piperidone ring surrounded by the positively charged residue LYS-866 is also understood from a CPH developed from 3D QSAR, where the nitrogen in the substituent is acting as the hydrophobic site (H) and the nitrogen in the piperidone ring is acting as a hydrogen bond donor with positive charge (P) as shown in Fig. 1. Benzimidazole ring is surrounded by hydrophobic residues like ILE-886, ILE-890, ILE-1042, VAL-896, CYS-1043 and LEU-887 indicates its role in hydrophobic interaction; in 3D QSAR model ring residues (R) also suggests the same. The reference ligand forms hydrogen bonding with CYS-917 via -N- of quinazoline ring and a similar interaction is also shown by -N- of benzimidazole ring of all piperidone derivatives with GLU-883 through hydrogen bonding.

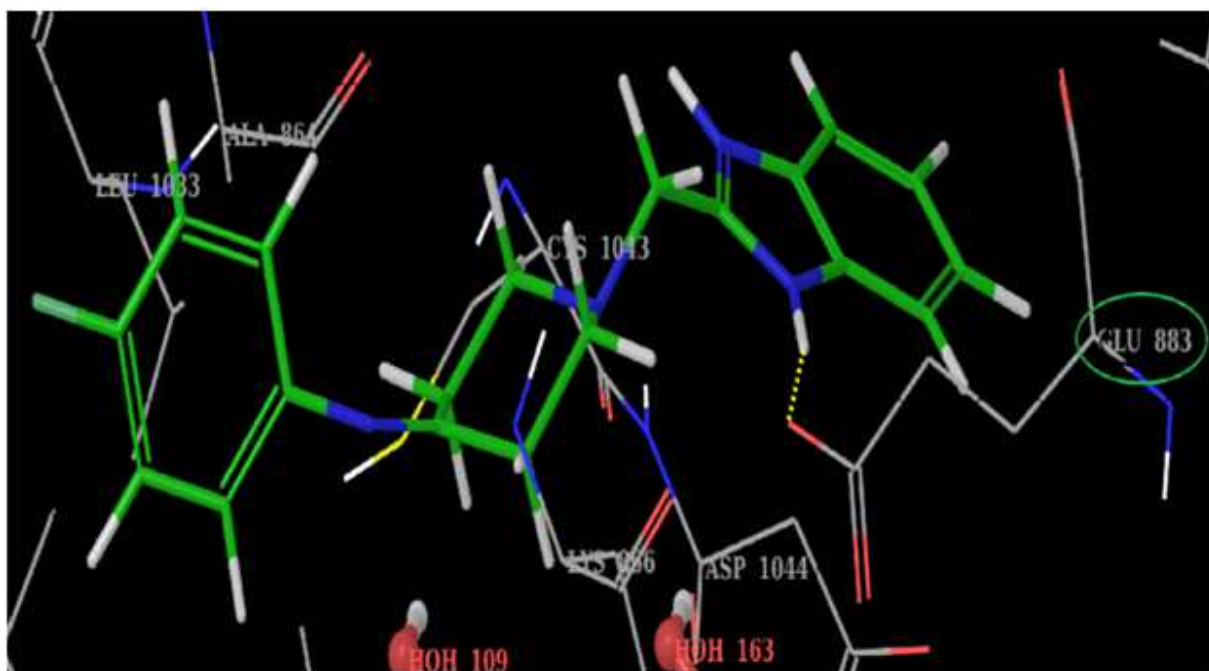


Figure 3: 3D Binding interaction of the compound, S6 in the active site of VEGFR-2 tyrosine kinase. H-bond interaction is indicated by dotted yellow bond with site residue (green ellipse).

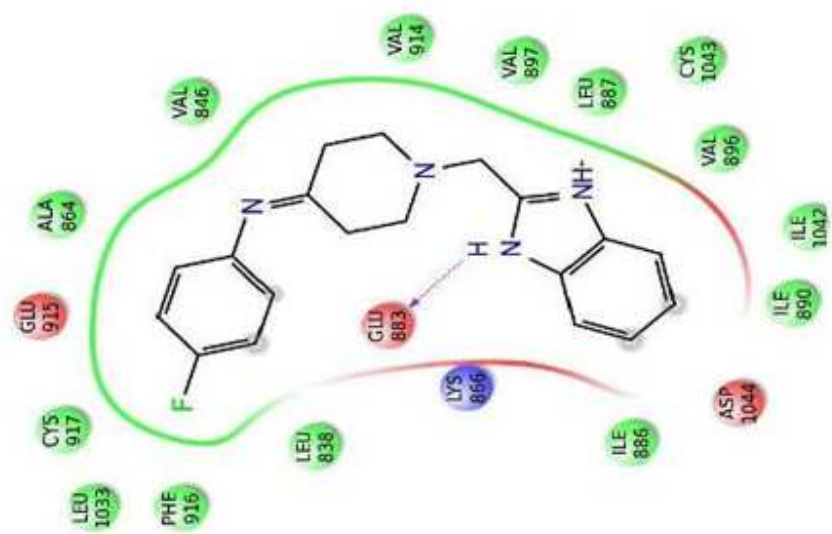


Figure 4: 2D binding interaction of S6 in the active site of VEGFR-2 tyrosine kinase.

Overall, the best model was Model 1 based on r^2 , q^2 , and RMSE and SD values as well as on the highest Pearson-R value. This pharmacophore model includes one hydrophobic (H), one hydrogen bond donor with positive ionic charge (P), and two aromatic rings (R). The pharmacophore hypothesis of angles, distances and alignment of all molecules are depicted in Fig. 1 and 2, respectively. The angles and distances between the four features are depicted in Table 3. For Model-1, the training set correlation is characterized by PLS factors ($r^2 = 0.7586$, $SD = 0.223$, $F = 20.4$). The test set correlation is characterized by PLS factors ($q^2 = 0.532$, $RMSE = 0.2509$, $Pearson-R = 0.7938$). The scattered plots of experimental versus predicted activity of training and test sets are depicted in Fig. 5.

Table 3 Distances and angles of pharmacophore hypothesis by Model-1

Hypothesis	Site1	Site2	Distance(A [*])	Hypothesis	Site 1	Site 2	Site 3	Angles (Degree)
HPRR.1	H4	P7	2.004	HPRR.1	P7	H4	R8	35.9
HPRR.1	H4	R8	4.928	HPRR.1	P7	H4	R9	48.1
HPRR.1	H4	R9	6.698	HPRR.1	R8	H4	R9	12.3
HPRR.1	P7	R8	3.507	HPRR.1	H4	P7	R8	124.6
HPRR.1	P7	R9	5.563	HPRR.1	H4	P7	R9	116.4
HPRR.1	R8	R9	2.155	HPRR.1	R8	P7	R9	8.4
				HPRR.1	H4	R8	P7	19.6
				HPRR.1	H4	R8	R9	138.6
				HPRR.1	P7	R8	R9	157.9
				HPRR.1	H4	R9	P7	15.6
				HPRR.1	H4	R9	R8	29.1
				HPRR.1	P7	R9	R8	13.7

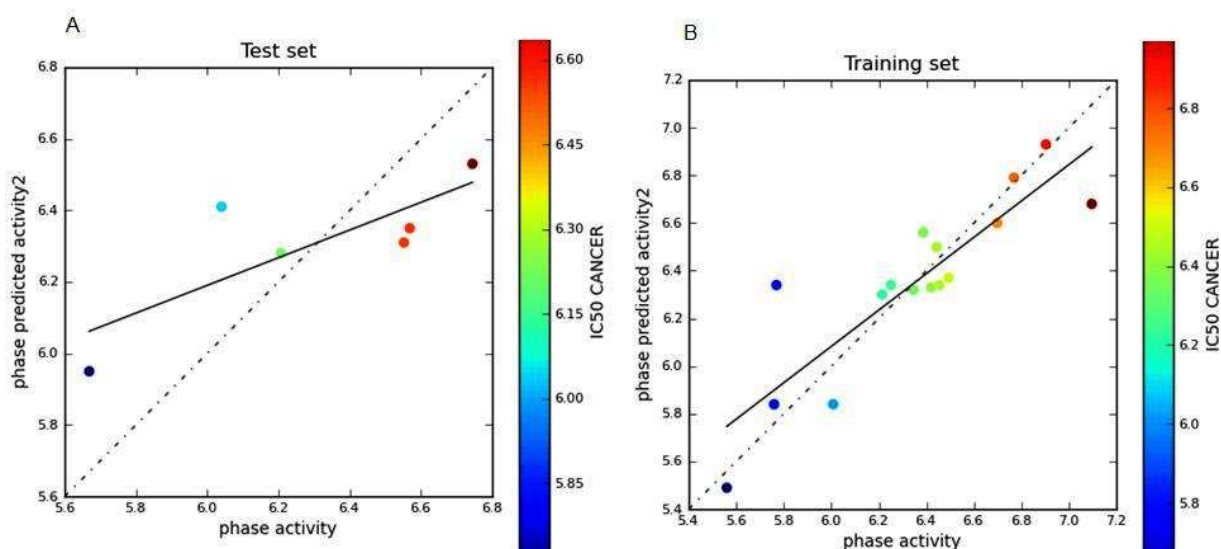


Figure 5: Scatter plots for the QSAR model applied to all compounds in the test (a) and training (b) set.

Reliable predictions could be obtained only from statistically significant valid QSAR models. The parameters r^2 , q^2 , SD, RMSE, and F are used to evaluate the robustness of a QSAR model. According to the reported method [23], Model 1 is validated as the best QSAR model, since the r^2 and q^2 values of model 1 are higher than those of Models 2, 3, 4 and 5. Moreover, RMSE value for Model 1 was found to be the lowest and the Pearson-R value was found to be the highest among other models. Further, by PHASE PLS analytical method, five various combinations of test and training sets were generated and evaluated. Compared to all other models consistent and good predictivity was observed for Model 1 for each combination. The predictive qualities of the QSAR models of all the molecules are satisfactory while considering the flexibility.

Correlation of the results of the docking study which was measured in terms of glide dock score values by comparing it with the docked poses of the reference ligand is shown in Table 1. The minimum glide dock score of -6.882, -6.536 and -6.323 kcal/mol of compound S6, S8 and S9 having dimethyl and dimethoxy phenyl and also fluorophenyl substituted derivatives proved that both electron donating and withdrawing groups substituted in the phenyl group favors the VEGFR-2 inhibition activity; but as the number of electron withdrawing groups increases in the phenyl group the activity decreases as it is evidenced from docking scores of compounds S11, S12, and S17.

CONCLUSION

Series of piperidone derivatives with anticancer activity against MCF7 cell lines were subjected to a 3D-QSAR study. Good statistical validation and predictabilities has been shown by all the developed 3D-QSAR models. Based on the PLS factors for training set ($r^2 = 0.7586$, SD = 0.223, F = 20.4) the for the test set ($q^2 = 0.532$, RMSE = 0.2509, Pearson-R = 0.7938) Model-1 (HPRR 1) was significantly more precise than other models. An insight into

the structure activity relationship has been provided by 3D-QSAR in terms of rational drug design. The importance of nitrogen in the substituent at the 4th position of piperidone ring is understood from a CPH developed from 3D QSAR where the nitrogen in the substituent is acting as the hydrophobic site (H). Nitrogen atom of the piperidone ring serves as hydrogen bond donor with positive charge (P7) in drug receptor interaction. Ring residue (R8, R9) in this model occupies much of the favorable position due to the presence of the hydrophobic benzimidazole ring. The bulky substituent is essential at the 4th position of the piperidone ring for producing VEGFR-2 kinase inhibition, it is also inferred from the docking results that the bulky moiety is located in a deep hydrophobic pocket formed by ALA-854, CYS-917, LEU-1033, PHE-916, LEU838 and VAL846. So this present study has provided us the guidance for further structural modification and development of potential VEGFR-2 tyrosine kinase inhibitors.

Acknowledgements

We are thankful to Manipal University for providing financial assistance to one of the authors (RR) and MCOPS, Manipal University for providing research facilities. We are grateful to Principal, PSG College of pharmacy, for providing facilities for molecular modeling studies. We gratefully acknowledge AICTE, DBT and DST, New Delhi, for providing analytical facilities to MCOPS through funding.

REFERENCES

- [1] I.S. Moreira, P.A. Fernandes, M.J. Ramos, *Anti-Cancer Agents Med. Chem.*, **2007**, 7, 223.
- [2] G. Bold, K.H. Altmann, J. Frei, M. Lang, P.W. Manley, P. Traxler, B. Wietfeld, J. Brügggen, E. Buchdunger, R. Cozens, S. Ferrari, P. Furet, F. Hofmann, G. Martiny-Baron, J. Mestan, J. Rösel, M. Sills, D. Stover, F. Acemoglu, E. Boss, R. Emmenegger, L. Lässer, E. Masso, R. Roth, C. Schlachter, W. Vetterli, *J. Med. Chem.*, **2000**, 43, 2310.
- [3] T. Kamba, D.M. McDonald, *Br. J. Cancer*, **2007**, 96, 1788.
- [4] R. van der Meel, M.H. Symons, R. Kudernatsch, R.J. Kok, R.M. Schiffelers, G. Storm, W.M. Gallagher, A.T. Byrne, *Drug Discov. Today*, **2011**, 16, 219.
- [5] T. Veikkola, M. Karkkainen, L. Claesson-Welsh, K. Alitalo, *Cancer Res.*, **2000**, 60, 203.
- [6] T. Takahashi, S. Yamaguchi, K. Chida, M. Shibuya, *EMBO J.*, **2001**, 20, 2768.
- [7] B.P. Eliceiri, R. Paul, P.L. Schwartzberg, J.D. Hood, J. Leng, D.A. Cheresh, *Mol. Cell.*, **1999**, 4, 915.
- [8] J. Rak, Y. Mitsuhashi, L. Bayko, J. Filmus, S. Shirasawa, T. Sasazuki, R.S. Kerbel, *Cancer Res.*, **1995**, 55, 4575.
- [9] L. Zhang, D. Yu, M. Hu, S. Xiong, A. Lang, L.M. Ellis, R.E. Pollock, *Cancer Res.*, **2000**, 60, 3655.
- [10] D. Shweiki, A. Itin, D. Soffer, E. Keshet, *Nature*, **1992**, 359, 843.
- [11] J. Hasan, R. Byers, G.C. Jayson, *Br. J. Cancer*, **2002**, 86, 1566.
- [12] L.E. Benjamin, D. Golijanin, A. Itin, D. Pode, E. Keshet, *J. Clin. Invest.*, **1999**, 103, 159.
- [13] G. Neufeld, T. Cohen, S. Gengrinovitch, Z. Poltorak, *FASEB J.*, **1999**, 13, 9.
- [14] J. Holash, S. Davis, N. Papadopoulos, S.D. Croll, L. Ho, M. Russell, P. Boland, R. Leidich, D. Hylton, E. Burova, E. Ioffe, T. Huang, C. Radziejewski, K. Bailey, J.P. Fandl, T. Daly, S.J. Wiegand, G.D. Yancopoulos, J.S. Rudge, *Proc. Natl. Acad. Sci. USA.*, **2002**, 99, 11393.
- [15] F. Elice, F. Rodeghiero, *Thromb. Res.*, **2010**, 125(Suppl 2), S55.
- [16] M.N. Noolvi, H.M. Patel, V. Bhardwaj, *Med. Chem.*, **2011**, 7, 200.
- [17] R. Darnag, M. E.L. Mazouz, A. Schmitzer, D. Villemin, A. Jarid, D. Cherqaoui, *Eur. J. Med. Chem.*, **2010**, 45, 1590.
- [18] R. Revathi, S.G. Kini, K.S.R. Pai, G. Arunkumar, *DUPHAT Dubai*, **2014**, P148.
- [19] N.R. Tawari, S. Bag, M.S. Degani, *J. Mol. Model.*, **2008**, 14, 911–21.
- [20] A. Golbraikh, M. Shen, Z. Xiao, Y.D. Xiao, K.H. Lee, A. Tropsha, *J. Comput. Aided Mol. Des.*, **2003**, 17, 241.
- [21] S.L. Dixon, A.M. Smondryev, E.H. Knoll, S.N. Rao, D.E. Shaw, R.A. Friesner, *J. Comput. Aided Mol. Des.*, **2006**, 20, 647.
- [22] H. Zhong, L.M. Tran, J.L. Stang, *J. Mol. Graph Mod.*, **2009**, 28, 336.
- [23] A. Tropsha, In: T.I. Oprea, (Ed.), *Chemoinformatics in drug discovery* (Wiley, Weinheim, **2005**) 437.